ISSN 1936-8798/$36.00
PUBLISHED BY ELSEVIER INC.
DOI: 10.1016/j.jcin.2010.09.022

CVN Interview

Difference of Culprit Lesion Morphologies Between ST-Segment Elevation Myocardial Infarction and Non–ST-Segment Elevation Acute Coronary Syndrome

An Optical Coherence Tomography Study

Yasushi Ino, MD, Takashi Kubo, MD, PhD, Atsushi Tanaka, MD, PhD, Akio Kuroi, MD, Hiroto Tsujioka, MD, Hideyuki Ikejima, MD, Keishi Okouchi, MD, Manabu Kashiwagi, MD, Shigeho Takarada, MD, PhD, Hironori Kitabata, MD, Takashi Tanimoto, MD, Kenichi Komukai, MD, Kohei Ishibashi, MD, Keizo Kimura, MD, PhD, Kumiko Hirata, MD, PhD, Masato Mizukoshi, MD, PhD, Toshio Imanishi, MD, PhD, Takashi Akasaka, MD, PhD

Wakayama, Japan

Objectives The aim of this study was to investigate the difference of culprit lesion morphologies assessed by optical coherence tomography (OCT) between ST-segment elevation myocardial infarction (STEMI) and non–ST-segment elevation acute coronary syndrome (NSTEACS).

Background Autopsy studies have reported that rupture of a thin-cap fibroatheroma and subsequent thrombus formation is the most important mechanism leading to acute coronary syndrome (ACS). Optical coherence tomography is a high-resolution imaging modality that is capable of investigating detailed coronary plaque morphology in vivo.

Methods We examined the culprit lesion morphologies by OCT in 89 consecutive patients with acute coronary syndrome (STEMI = 40; NSTEACS = 49).

Results The incidence of plaque rupture, thin-cap fibroatheroma, and red thrombus was significantly higher in STEMI compared with NSTEACS (70% vs. 47%, $p = 0.033$, 78% vs. 49%, $p = 0.008$, and 78% vs. 27%, $p < 0.001$, respectively). Although the lumen area at the site of plaque rupture was similar in the both groups (2.44 ± 1.34 mm^2 vs. 2.96 ± 1.91 mm^2, $p = 0.250$), the area of ruptured cavity was significantly larger in STEMI compared with NSTEACS (2.52 ± 1.36 mm^2 vs. 1.67 ± 1.37 mm^2, $p = 0.034$). Furthermore, the ruptured plaque of which aperture was open-wide against the direction of coronary flow was more often seen in STEMI compared with NSTEACS (46% vs. 17%, $p = 0.036$).

Conclusions The present OCT study demonstrated the differences of the culprit lesion morphologies between STEMI and NSTEACS. The morphological feature of plaque rupture and the intracoronary thrombus could relate to the clinical presentation in patients with acute coronary disease. (J Am Coll Cardiol Intv 2011;4:76–82) © 2011 by the American College of Cardiology Foundation

From the Department of Cardiovascular Medicine, Wakayama Medical University, Wakayama, Japan. Drs. Akasaka and Kubo were supported in part by a Grant-in-Aid from the Ministry of Education, Culture, Sports, Science and Technology of Japan. All other authors have reported that they have no relationships to disclose.

Manuscript received May 24, 2010; revised manuscript received August 12, 2010, accepted September 17, 2010.

Rupture of vulnerable plaque with subsequent thrombus formation is a major cause of acute coronary syndrome (ACS). The pathological characteristics of vulnerable plaques include a thin fibrous cap with macrophage infiltration and a large lipid core (1,2). The traditional paradigm is that the mechanism of plaque rupture is identical between ST-segment elevation myocardial infarction (STEMI) and

See page 83

non–ST-segment elevation acute coronary syndrome (NSTEACS), with some clots being partially or totally occlusive. Intravascular ultrasound (IVUS) studies reported that the morphology of plaque rupture site might affect obstructive thrombus formation (3–6). However, the relatively coarse resolution of IVUS precludes detailed assessment of the ruptured plaque, including fibrous cap thickness and ruptured cavity size.

Optical coherence tomography (OCT) is a high-resolution (approximately 10 to 20 μm) imaging modality, which is approximately 10 times higher than IVUS. Optical coherence tomography is a feasible and safe imaging modality in patients with ACS and allows us to identify plaque ruptures, thin-cap fibroatheromas (TCFAs) and intracoronary thrombus in vivo (7–12). We used OCT to compare culprit lesion morphologies between STEMI and NSTEACS.

Methods

Study population. We enrolled 104 consecutive ACS patients (STEMI = 48, NSTEACS = 56) with de novo culprit lesion in the native coronary artery who were admitted to Wakayama Medical University Hospital and underwent coronary angiography (CAG) between July 2008 and March 2009. The enrollment criteria of STEMI in this study was based on the concurrence of all the following: 1) continuous chest pain for at least 30 min; 2) arrival at our hospital within 6 h from the onset of the symptom; 3) ST-segment elevation ≥0.1 mV in 2 or more contiguous leads on 12-lead electrocardiogram; 4) elevated myocardial enzymes (plasma creatine kinase and creatine kinase-myocardial band fraction levels more than 2 times higher than normal); and 5) an identifiable culprit lesion in a native coronary artery by CAG. Criteria for NSTEACS include non-STEMI and unstable angina. The criteria of non-STEMI in this study was based on the concurrence of all the following: 1) new findings of ST-segment depression >0.1 mm or T-wave inversion >0.4 mm in 2 or more contiguous leads; 2) symptoms consistent with acute myocardial infarction; and 3) the presence of elevated levels of troponin T (>0.1 ng/ml). Unstable angina was defined as an unstable pattern of chest pain (at rest, new onset, or crescendo angina) coinciding with objective evidence of CAG, demonstrating a >50% coronary stenosis but without significant elevation in troponin T (>0.1 ng/ml). Patients with cardiogenic shock, renal insufficiency with baseline serum creatinine >2.0 mg/dl, a left main coronary artery lesion, an extremely tortuous vessel, and a reference vessel diameter of >4 mm were excluded because of the potential difficulty in performing and interpreting the OCT findings in such situations. This protocol was approved by the Wakayama Medical University Ethics Committee, and all patients provided informed consent before participation.

Study protocol. Oral aspirin (162 mg) and intravenous heparin (100 U/kg) were administered before coronary intervention. Thrombolysis was not performed for any patient. The culprit lesion was identified on the basis of the findings by a CAG as well as an electrocardiogram and transthoracic echocardiogram. In patients with Thrombolysis In Myocardial Infarction (TIMI) flow grade ≤2, aspiration thrombectomy was performed by a 5.1-F aspiration catheter (Export Catheter, Medtronic, Japan, Tokyo, Japan) before OCT imaging, but pre-dilation by balloon catheter was not allowed. After reperfusion with TIMI flow grade 3, the culprit lesion was observed by OCT as described previously (8,11). Briefly, a 0.016-inch OCT catheter (ImageWire, LightLab Imaging, Westford, Massachusetts) was advanced to the distal end of the culprit lesion through a 3-F occlusion balloon catheter (Helious, Goodman Co., Ltd., Nagoya, Japan). To remove the blood from the field of view, occlusion balloon was inflated to 0.4 to 0.6 atm at the proximal site of the culprit lesion, and a mixture of commercially available dextran 40 and Lactated Ringer's solution (low-molecular-weight Dextran L Injection, Otsuka Pharmaceutical Factory, Tokushima, Japan) was infused into the coronary artery from the distal tip of the occlusion balloon catheter at 0.5 ml/s.

Abbreviations and Acronyms

ACS = acute coronary syndrome
CAG = coronary angiography
CSA = cross-sectional area
IVUS = intravascular ultrasound
NSTEACS = non–ST-segment elevation acute coronary syndrome
OCT = optical coherence tomography
QCA = quantitative coronary angiographic analysis
ROC = receiver-operator characteristic
STEMI = ST-segment elevation myocardial infarction
TCFA = thin-cap fibroatheroma

For the assessment of the proximal coronary artery lesions, we used a continuous-flushing (nonocclusive) technique of OCT image acquisition, which is a newly developed alternative to the balloon-occlusion technique (11,13). To flush the vessel, we infused a mixture of commercially available dextran 40 and lactated Ringer's solution direct from the guiding catheter at a rate of 2.5 to 4.5 ml/s with an injector pump (Mark V, Medrad, Inc., Warrendale, Pennsylvania). Regardless of the OCT technique used, in all

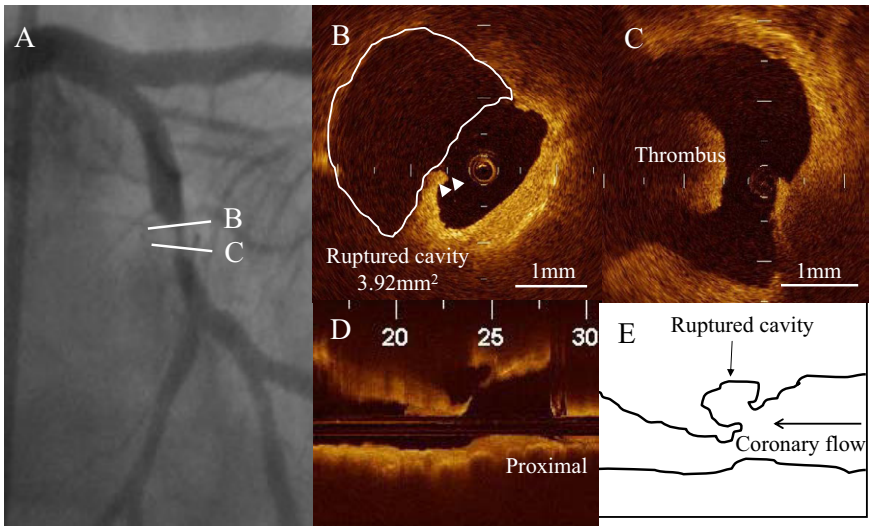

Figure 1. Representative Case With ST-Segment Elevation Myocardial Infarction

(A) Coronary angiography demonstrated a complex lesion in the mid portion of the left circumflex artery. **(B)** The large ruptured cavity and residual fibrous cap **(arrowheads)** was observed by optical coherence tomography (OCT) in the infarct-related lesion. **Scale bar** = 1 mm. **(C)** The OCT detected a red thrombus that was characterized as high-backscattering protrusion with signal-free shadow. **(D)** The longitudinal OCT image revealed proximal-type rupture. The aperture of a ruptured plaque is open-wide against the direction of coronary flow. **(E)** Scheme of the longitudinal OCT image.

cases, the culprit lesion was imaged with an automatic pullback device traveling at 1 mm/s. The OCT images were digitalized and analyzed by a musical instrument digital interface to control voltage converter OCT console.

OCT image analysis. All OCT images were analyzed by 2 independent investigators (Y.I. and T.K.) who were blinded to the angiographic data and clinical presentations. When there was any discordance between the observers, a consensus reading was obtained. Presence of plaque rupture, intracoronary thrombus, or TCFA was noted. Plaque rupture was defined as the presence of fibrous-cap discontinuity and a cavity formation in the plaque. The lumen cross-sectional area (CSA) and the ruptured cavity CSA were measured at the site of largest intra-plaque cavity (Figs. 1B and 2B). The minimum lumen CSA was also estimated. The longitudinal morphological features of plaque rupture were classified into 3 types according to the previous IVUS report (6). Proximal-type rupture was defined as the ruptured plaque of which aperture was open-wide against the direction of coronary flow (Figs. 1D and 1E). Distal-type rupture was defined as the ruptured plaque of which aperture opened along the direction of coronary flow (Figs. 2D and 2E). Mid-type rupture was defined as the ruptured plaque of which aperture opened at the center of the plaque. Intracoronary thrombus was identified as a mass that protruded into the vessel lumen from the surface of the vessel wall. Red thrombus, which is considered a fresh one and mainly consists of red blood cell (14), was defined as high-backscattering protrusions inside the lumen of the artery with signal-free shadowing in the OCT image (15) (Fig. 1C). White thrombus, which is considered an older one in the process of thrombus organization and mainly consists of platelet and fibrin (14), was defined as low-backscattering protrusions with signal-rich one according to a previous report (15) (Fig. 2C). Maximal lipid arc was semiquantified according to the number of involved quadrants on the cross-sectional OCT image. When lipid was present in 2 quadrants in any of the images within a plaque, the plaque was deemed to be lipid-rich. A fibrous cap was identified as a signal-rich homogenous region overlying a lipid core, which was characterized by a signal-poor region on the OCT image. The thinnest part of the fibrous cap was measured 3 times, and the average value was calculated. The lesion with a fibrous cap of <65 μm was diagnosed as TCFA.

Angiographic analysis. The CAG was performed after the administration of 0.2 mg intracoronary nitroglycerin. With the guiding catheter for magnification calibration, quantitative coronary angiographic analysis (QCA) was performed with a validated automated edge detection algorithm (QCA-CMS version 5.0, Medis, Leiden, the Netherlands) by 2 independent observers (H.K. and T.T.) blinded to the clinical information including OCT findings. Angiographic morphology in the culprit lesion was classified as either simple or complex on the basis of the American College of Cardiology/American Heart Association classification (16) and the Ambrose classification (17,18). Simple lesions were concentric or eccentric and characterized by a smooth border and a broad neck. Complex lesions were eccentric with a narrow neck, irregular borders, or overhanging edges,

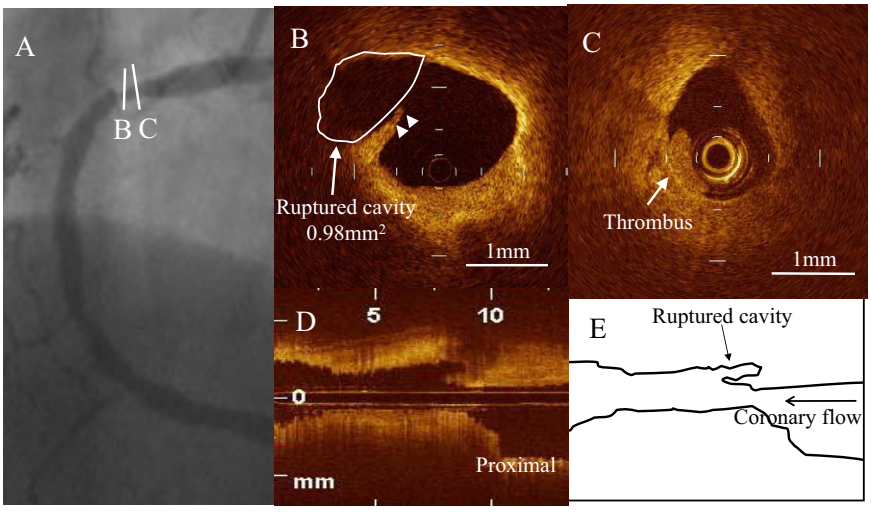

Figure 2. Representative Case With Non–ST-Segment Elevation Acute Coronary Syndrome

(A) Coronary angiography demonstrated a severe stenosis in the proximal portion of the right coronary artery. **(B)** The small ruptured cavity and residual fibrous cap **(arrows and arrowheads)** was observed by optical coherence tomography (OCT) in the culprit lesion. **Scale bar** = 1 mm. **(C)** The OCT detected a white thrombus that was characterized as signal-rich and low-backscattering protrusion. **(D)** The longitudinal OCT image revealed distal-type rupture. The aperture of a ruptured plaque is open along the direction of coronary flow. **(E)** Scheme of the longitudinal OCT image.

including ulceration, the presence of thrombus, or total occlusion. Ulceration was defined as a small crater consisting of a discrete luminal widening with luminal irregularity. Intracoronary thrombus was defined as a filling defect seen in multiple projections.

Statistical analysis. Stat View 5.0 software (SAS Institute, Inc., Cary, North Carolina) was used to perform all statistical analyses except receiver-operator characteristic (ROC) curve analysis, which was performed with SPSS software, version 11.0 (SPSS, Inc., Chicago, Illinois). Categorical variables were presented as frequencies, with comparison with chi-square statistics or Fisher exact test (if the expected cell value was <5). Continuous variables were presented as the mean ± SD and were compared with unpaired Student *t* tests. The ROC curve analysis was used to compare the quantitative OCT variables for predicting STEMI. A p value <0.05 was considered statistically significant.

Results

Baseline clinical characteristics. We excluded, of the 104 patients with STEMI or NSTEACS, 2 patients with left main coronary artery lesion, 3 patients with renal insufficiency, 5 patients with cardiogenic shock, and 5 patients with inadequate OCT image acquisition. Thus, 89 patients (STEMI = 40 and NSTEACS = 49) were assessed in the present study.

Baseline clinical characteristics are shown in Table 1. There were no differences in the variables of baseline clinical characteristics between STEMI and NSTEACS, except for left ventricular ejection fraction (p = 0.005). The median elapsed time in STEMI (time from the onset to OCT imaging) and NSTEACS (time from the latest heart attack to OCT imaging) was 3.9 h and 14.5 h, respectively (p < 0.001). The nonocclusive technique was performed in 24 (27%) patients (STEMI = 9 and NSTEACS = 15).

Angiographic findings. Angiographic findings are shown in Table 2. A TIMI flow grade 0 (p < 0.001), complex lesion (p < 0.006), and angiographic thrombus (p < 0.001) were more often seen in STEMI compared with NSTEACS. Minimum lumen diameter was smaller (0.36 ± 0.39 mm vs. 0.69 ± 0.42 mm, p < 0.001) and percentage diameter stenosis was greater (89 ± 11% vs. 79 ± 11%, p < 0.001)

Table 1. Baseline Clinical Characteristics

	STEMI (n = 40)	NSTEACS (n = 49)	p Value
Age, yrs	66 ± 13	63 ± 10	0.209
Male	30 (75)	41 (84)	0.427
Hypertension	25 (63)	25 (51)	0.293
Dyslipidemia	20 (50)	31 (63)	0.282
Diabetes mellitus	17 (42)	14 (29)	0.187
Cigarette smoking	22 (55)	19 (39)	0.141
Prior PCI	2 (5)	9 (18)	0.103
Multivessel disease	16 (40)	14 (29)	0.271
LVEF, %	53 ± 9	59 ± 10	0.005

Values are given as n (%) or mean ± SD.

LVEF = left ventricular ejection fraction; NSTEACS = non–ST-segment elevation acute coronary syndrome; PCI = percutaneous coronary intervention; STEMI = ST-segment elevation myocardial infarction.

Table 2. Angiographic Findings

	STEMI (n = 40)	NSTEACS (n = 49)	p Value
Culprit vessel			
LAD/LCX/RCA	11/9/2020	22/7/2020	0.219
TIMI flow grade			
0/1/2/3	22/2/10/6	2/2/11/34	<0.001
Culprit lesion characteristics			0.006
Simple lesion	2 (5)	17 (35)	
Complex lesion	38 (95)	32 (75)	
Ulceration	10 (25)	8 (16)	0.427
Thrombus	29 (73)	5 (10)	<0.001
QCA results			
Reference vessel diameter, mm	3.32 ± 0.57	3.16 ± 0.40	0.125
Minimum lumen diameter, mm	0.36 ± 0.39	0.69 ± 0.42	<0.001
Percent diameter stenosis, %	89 ± 11	79 ± 11	<0.001

Values are given as n (%) or mean ± SD.
LAD = left anterior descending; LCX = left circumflex; QCA = quantitative coronary angiography; RCA = right coronary artery; TIMI = Thrombolysis In Myocardial Infarction; other abbreviations as in Table 1.

in STEMI than in NSTEACS. Aspiration thrombectomy was more often performed in STEMI than in NSTEACS (88% vs. 14%, $p < 0.001$).

OCT findings. Representative OCT images are shown in Figure 1 (STEMI) and Figure 2 (NSTEACS). The OCT findings are summarized in Table 3. Plaque rupture (70% vs. 47%, $p = 0.033$), lipid-rich plaque (90% vs. 71%, $p = 0.036$), TCFA (78% vs. 49%, $p = 0.008$), and red thrombus (78% vs. 27%, $p < 0.001$) were more often seen in STEMI compared with NSTEACS. The fibrous cap thickness was significantly thinner in STEMI than that in NSTEACS (55 ± 20 μm vs. 109 ± 55 μm, $p < 0.001$). The OCT findings of ruptured plaques are shown in Table 4. The maximum ruptured cavity CSA was larger in STEMI than in NSTEACS (2.52 ± 1.36 mm^2 vs. 1.67 ± 1.37 mm^2, $p = 0.034$). The lumen CSA at the site of maximum ruptured cavity CSA (2.44 ± 1.34 mm^2 vs. 2.96 ± 1.91 mm^2, $p = 0.250$) and the minimum lumen CSA (1.95 ± 0.80 mm^2 vs. 1.88 ± 0.86 mm^2, $p = 0.756$) were similar in the both groups. Compared with the minimum lumen CSA site, the maximal ruptured cavity was more often located proximally in STEMI (64% vs. 35%, $p = 0.036$) and distally in NSTEACS (11% vs. 39%, $p = 0.017$). Furthermore, proximal-type rupture was more often seen in STEMI (46% vs. 17%, $p = 0.039$), and distal-type rupture was more often observed in NSTEACS (11% vs. 35%, $p = 0.048$). The ROC curves of the quantitative OCT variables are shown in Figure 3. The areas under the curve of maximum ruptured cavity CSA, lumen CSA at the maximum ruptured cavity site, minimum lumen CSA, and minimum fibrous cap thickness for predicting STEMI were 0.718, 0.473, 0.542, and 0.407, respectively.

Table 3. OCT Findings of Culprit Lesions

	STEMI (n = 40)	NSTEACS (n = 49)	p Value
Plaque rupture	28 (70)	23 (47)	0.033
Lipid-rich plaque	36 (90)	35 (71)	0.036
Fibrous cap thickness, μm	55 ± 20	109 ± 55	<0.001
TCFA	31 (78)	24 (49)	0.008
Thrombus	40 (100)	32 (65)	<0.001
Red thrombus	31 (78)	13 (27)	<0.001
White thrombus	9 (22)	19 (39)	0.114

Values are given as n (%) or mean ± SD.
TCFA = thin-cap fibroatheroma; other abbreviations as in Tables 1 and 2.

Table 4. OCT Findings of Ruptured Plaques

	STEMI (n = 28)	NSTEACS (n = 23)	p Value
Maximum ruptured cavity CSA, mm^2	2.52 ± 1.36	1.67 ± 1.37	0.034
Lumen CSA at maximum ruptured cavity site, mm^2	2.44 ± 1.34	2.96 ± 1.91	0.250
Minimum lumen CSA, mm^2	1.95 ± 0.80	1.88 ± 0.86	0.756
Location of the maximum ruptured cavity			
Proximal to the minimum lumen CSA site	18 (64)	8 (35)	0.036
Same with the minimum lumen CSA site	7 (25)	6 (26)	0.929
Distal to the minimum lumen CSA site	3 (11)	9 (39)	0.017
Longitudinal morphological features of plaque rupture			
Proximal-type	13 (46)	4 (17)	0.039
Mid-type	12 (43)	11 (48)	0.782
Distal-type	3 (11)	8 (35)	0.048

Values are given as n (%) or mean ± SD.
CSA = cross-sectional area; OCT = optical coherence tomography; other abbreviations as in Table 1.

Discussion

The present OCT study demonstrated the differences of the culprit lesion morphologies between STEMI and NSTEACS. The main findings were summarized as follows: 1) plaque rupture, TCFA, and red thrombus were more often seen in STEMI; 2) the size of ruptured cavity was greater in STEMI; and 3) the ruptured plaque of which aperture was open-wide against the direction of coronary flow was more often seen in STEMI. Our results suggest that these plaque morphologies in the culprit lesion might affect the clinical presentations in patients with ACS.

Plaque rupture and ACS. Plaque rupture with subsequent thrombus formation is the most frequent cause of ACS (1,2). Pathological studies showed that plaque rupture was seen in 70% of patients with coronary artery disease who

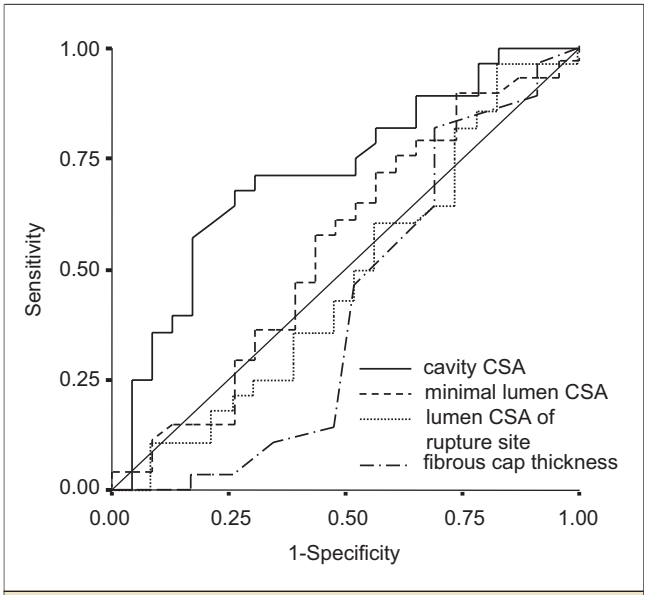

Figure 3. Receiver-Operator Characteristic Curve Analysis of Quantitative Optical Coherence Tomography Variables for Predicting STEMI

The areas under the curve of maximum ruptured cavity cross-sectional area (CSA), lumen CSA at the maximum ruptured cavity site, minimum lumen CSA, and minimum fibrous cap thickness for predicting ST-segment elevation myocardial infarction (STEMI) were 0.718, 0.473, 0.542, and 0.407, respectively.

died suddenly (1). The IVUS studies demonstrated that the prevalence of plaque rupture was 59% to 66% in the culprit lesion of ACS (3,19). Angioscopic studies also reported that the prevalence of plaque rupture was 56% in patients with ACS (20). Furthermore, postmortem examinations (21) and IVUS studies (5) disclosed that smaller lumens and evidence of thrombus are the important risks linking ruptured plaques to ACS. The traditional paradigm is that the mechanism of plaque rupture is identical between STEMI and NSTEACS, with some clots being partially or totally occlusive. However, it is not clear why some plaque ruptures lead to STEMI, whereas others cause NSTEACS. We used OCT to compare culprit lesion morphologies between STEMI and NSTEACS. The micron-scale resolution of OCT has an ability to capture in vivo what was previously seen only through the microscope of a pathologist. Early in vitro and in vivo studies have demonstrated the possibility that OCT might identify vulnerable plaque features (7–12,22). In the present OCT analysis, the incidence of plaque rupture, TCFA, and red thrombus was significantly higher in STEMI than in NSTEACS. Moreover, the ruptured cavity CSA was significantly greater in STEMI compared with NSTEACS. An exposure of necrotic core induced by plaque rupture could lead to the contact of thrombogenic lipid content with flowing blood. Our results suggest that the size of the underlying lipid pool or necrotic core might relate to post-plaque rupture thrombus formation and clinical presentations of ACS.

Longitudinal morphology of plaque rupture. Not only the cross-sectional feature but also the longitudinal morphology of plaque rupture affects the coronary flow, which is closely related to obstructive thrombus formation. In a previous 3-dimensional IVUS study we demonstrated that the ACS patients with plaque rupture in the proximal shoulder site showed TIMI flow grade 0 on the initial angiogram more frequently than those with plaque rupture in the midportion or distal shoulder site (proximal type, 86%; mid-type, 50%; and distal type, 31%; $p = 0.002$) (6). In the proximal-type rupture, antegrade coronary flow causes the flap of the ruptured plaque to "roll up" back across the rupture site, extending the aperture of the ruptured plaque. Then, more of the thrombogenic contents in the lipid core are exposed to coronary flow, compared with other rupture types. This wider exposure of the plaque contents might result in more rapid thrombus formation and even total occlusion of the coronary artery. In the present analysis of longitudinally reconstructed OCT images, plaque rupture in the proximal shoulder site was more often seen in STEMI than in NSTEACS. Our results suggest that the longitudinal morphology of plaque rupture might be an important determinant of coronary artery occlusion and clinical presentations of ACS.

Study limitations. The present study had several limitations. First, aspiration thrombectomy was performed before OCT imaging in patients with TIMI flow grade ≤2. A thrombectomy catheter might have modified the culprit lesion morphologies and induced the cavity opening against the flow direction. Second, thrombus might affect analysis of the plaque behind, making it especially difficult to observe plaque rupture and erosion. Third, the histological examination was not performed in the materials obtained by aspiration thrombectomy. Fourth, the relatively shallow imaging depth of the current time-domain OCT precludes the assessment of plaque burden and arterial positive remodeling, which are well-described characteristics of vulnerable plaque (1). A second-generation OCT technology, termed Fourier-domain OCT, might eliminate these technical limitations of the present study (9,23). Finally, the study population was relatively small. Therefore, the present results should be viewed as preliminary and await confirmation by larger clinical trials with a second-generation OCT use.

Conclusions

The present OCT study demonstrated the higher incidence of plaque rupture in STEMI than in NSTEACS. Moreover, the size of ruptured cavity was greater in STEMI, and the ruptured plaque of which aperture was open-wide against the direction of coronary flow was more often observed in STEMI compared with NSTEACS. The morphological feature of plaque rupture might relate to subse-

JACC: CARDIOVASCULAR INTERVENTIONS, VOL. 4, NO. 1, 2011
JANUARY 2011:76–82

quent thrombus formation and clinical presentation in patients with acute coronary disease.

Reprint requests and correspondence: Dr. Takashi Akasaka, Department of Cardiovascular Medicine, Wakayama Medical University, 811-1 Kimiidera, Wakayama 641-8509, Japan. E-mail: akasat@wakayama-med.ac.jp.

REFERENCES

1. Virmani R, Kolodgie FD, Burke AP, Farb A, Schwartz SM. Lessons from sudden coronary death: a comprehensive morphological classification scheme for atherosclerotic lesions. Arterioscler Thromb Vasc Biol 2000;20:1262–75.
2. Falk E, Shah PK, Fuster V. Coronary plaque disruption. Circulation 1995;92:657–71.
3. Kusama I, Hibi K, Kosuge M, et al. Impact of plaque rupture on infarct size in ST-segment elevation anterior acute myocardial infarction. J Am Coll Cardiol 2007;50:1230–7.
4. Maehara A, Mintz GS, Bui AB, et al. Morphologic and angiographic features of coronary plaque rupture detected by intravascular ultrasound. J Am Coll Cardiol 2002;40:904–10.
5. Fujii K, Kobayashi Y, Mintz GS, et al. Intravascular ultrasound assessment of ulcerated ruptured plaques: a comparison of culprit and nonculprit lesions of patients with acute coronary syndromes and lesions in patients without acute coronary syndromes. Circulation 2003;108:2473–8.
6. Tanaka A, Shimada K, Namba M, et al. Relationship between longitudinal morphology of ruptured plaques and TIMI flow grade in acute coronary syndrome: a three-dimensional intravascular ultrasound imaging study. Eur Heart J 2008;29:38–44.
7. Jang IK, Tearney GJ, MacNeill B, et al. In vivo characterization of coronary atherosclerotic plaque by use of optical coherence tomography. Circulation 2005;111:1551–5.
8. Kubo T, Imanishi T, Takarada S, et al. Assessment of culprit lesion morphology in acute myocardial infarction: ability of optical coherence tomography compared with intravascular ultrasound and coronary angioscopy. J Am Coll Cardiol 2007;50:933–9.
9. Kubo T, Akasaka T. Optical coherence tomography imaging: current status and future perspectives. Cardiovasc Interv Ther 2010;25:2–10.
10. Bezerra HG, Costa MA, Guagliumi G, Rollins AM, Simon DI. Intracoronary optical coherence tomography: a comprehensive review clinical and research applications. J Am Coll Cardiol Intv 2009;2:1035–46.
11. Tanaka A, Imanishi T, Kitabata H, et al. Morphology of exertion-triggered plaque rupture in patients with acute coronary syndrome: an optical coherence tomography study. Circulation 2008;118:2368–73.
12. Kubo T, Imanishi T, Takarada S, et al. Comparison of vascular response after sirolimus-eluting stent implantation between unstable angina pectoris and stable angina pectoris: a serial optical coherence tomography study. J Am Coll Cardiol Img 2008;1:475–84.
13. Prati F, Cera M, Ramazzotti V, et al. From bench to bedside: a novel technique of acquiring OCT images. Circ J 2008;72:839–43.
14. Takano M, Inami S, Ishibashi F, et al. Angioscopic follow-up study of coronary ruptured plaques in nonculprit lesions. J Am Coll Cardiol 2005;45:652–8.
15. Kume T, Akasaka T, Kawamoto T, et al. Assessment of coronary arterial thrombus by optical coherence tomography. Am J Cardiol 2006;97:1713–7.
16. Ellis SG, Vandormael MG, Cowley MJ, et al. Coronary morphologic and clinical determinants of procedural outcome with angioplasty for multivessel coronary artery disease: implications for patient selection. Circulation 1990;82:1193–202.
17. Ambrose JA, Winters SL, Stern A, et al. Angiographic morphology and the pathogenesis of unstable angina pectoris. J Am Coll Cardiol 1985;5:609–16.
18. Ambrose JA, Winters SL, Arora RR, et al. Coronary angiographic morphology in myocardial infarction: a link between the pathogenesis of unstable angina and myocardial infarction. J Am Coll Cardiol 1985;6:1233–8.
19. Hong MK, Mintz GS, Lee CW, et al. Comparison of coronary plaque rupture between stable angina and acute myocardial infarction: a 3-vessel intravascular ultrasound study in 235 patients. Circulation 2004;110:928–33.
20. Mizote I, Ueda Y, Ohtani T, et al. Distal protection improved reperfusion and reduced left ventricular dysfunction in patients with acute myocardial infarction who had angioscopically defined ruptured plaque. Circulation 2005;112:1001–7.
21. Qiao JH, Fishbein MC. The severity of coronary atherosclerosis at sites of plaque rupture with occlusive thrombosis. J Am Coll Cardiol 1991;17:1138–42.
22. Kubo T, Imanishi T, Takarada S, et al. Implication of plaque color classification for assessing plaque vulnerability: a coronary angioscopy and optical coherence tomography investigation. J Am Coll Cardiol Intv 2008;1:74–80.
23. Takarada S, Imanishi T, Liu Y, et al. Advantage of next-generation frequency-domain optical coherence tomography compared with conventional time-domain system in the assessment of coronary lesion. Catheter Cardiovasc Interv 2010;75:202–6.

Key Words: acute coronary syndrome ■ optical coherence tomography ■ plaque morphology ■ plaque rupture ■ thin-cap fibroatheroma.